

unequal. It was shown that the redistribution of the stresses in this case may result in a significant decrease of the maximum tension stresses in the specimen.

#### LITERATURE CITED

1. V. S. Bakunov, D. N. Poluboyarinov, R. Ya. Popil'skii, et al., *Ogneupory*, No. 10, 45-49 (1969).
2. I. I. Vishnevskii, E. I. Aksel'rod, and N. D. Tal'yanskaya, *Ogneupory*, No. 8, 60-66 (1973).
3. S. J. Warshaw and F. H. Norton, *J. Am. Ceram. Soc.*, **45**, No. 10, 479-486 (1962).
4. W. D. Kingery, *Kinetics of High-Temperature Processes*, MIT Press (1959).
5. W. L. Barmore and R. R. Vandervoort, *J. Am. Ceram. Soc.*, **48**, No. 10, 499-505 (1965).
6. N. N. Malinin, *Applied Theory of Plasticity and Creep* [in Russian], Mashinostroenie, Moscow (1968).

#### THE DEFORMABILITY CHARACTERISTICS AS A FACTOR IN THE CALCULATION OF THE CRITERIA OF THE THERMAL-SHOCK RESISTANCE OF REFRACTORIES

G. A. Gototsi

UDC 666.76.017:620.179.13

The numerous cases where the analytically predicted thermal-shock resistance of refractories differs from the experimental results are evidence of the unreliability of the analytical methods used when deciding on refractory products for practical purposes. An analysis of the sources of this discrepancy [1, 2] showed that to increase the reliability of the analytical prediction it is necessary to take into account not only the conditions in which the thermal load is applied to the material but also any difference there may be between the characteristics of its actual behavior under a thermal load and the assumed characteristics upon which the derivation of the criterion being used is based.

It is known [1, 3] that nearly all conventional criteria of thermal-shock resistance are based on the assumption that the elasticity of the materials varies linearly right up to the instant of destruction whereas many refractories of a heterogeneous structure exhibit inelastic deformation at high and even normal temperatures [4, 5].

In this article the criteria of thermal-shock resistance are defined more precisely in order to arrive at a more reliable assessment of the ability of refractory materials to resist the effects of thermal action. It was shown earlier [3] that the criterion of thermal-shock resistance, which defines the resistance of a material to cracking on the basis of the theory of maximum stresses, can be written as follows:

$$A = \frac{\sigma_u}{E\alpha} B, \quad (1)$$

where  $\sigma_u$  is the ultimate strength;  $E$ , the elastic modulus;  $\alpha$ , the coefficient of linear thermal expansion; and  $B$ , a parameter which expresses the characteristics of the formation of uneven temperature fields.

The criterion of thermal-shock resistance based on the statistical theory of strength [6, p. 643] can be easily expressed in the same form in which case the parameter  $B$  will take into account also the statistical characteristics of the material.

The ratio  $\sigma_u/E\alpha$  from Eq. (1) sometimes called the  $R$  criterion, describes the resistance to thermal deformation and expresses the logical assumption, which agrees with the theory of thermoelasticity, that when the deformability of the material is high ( $\sigma_u/E$  is the limiting deformation according to Hooke's law) and its coefficient of linear thermal expansion low its thermal-shock resistance will be high.

The criterion [7] which expresses the resistance to cracking is based on a logical assumption which agrees

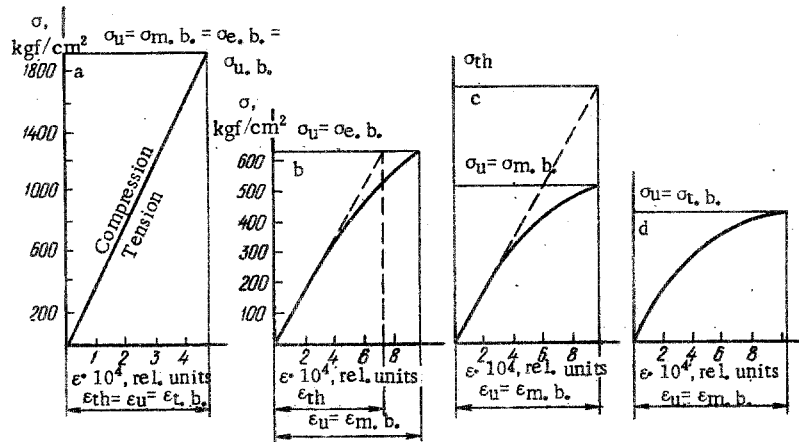


Fig. 1. Diagrams of deformation in bending: a) translucent corundum ( $\text{Al}_2\text{O}_3 + 0.1\% \text{MgO}$ ); b, c, and d) zircon-containing corundum ( $\text{Al}_2\text{O}_3 + 15\% \text{ZrSiO}_4$ );  $\sigma_u$ , ultimate compression strength;  $\sigma_{m.b.}$ , ultimate strength calculated with account taken of the nonlinearity of the deformation diagram of the material (mean bending strength);  $\sigma_{e.b.}$ , ultimate strength calculated for the linear elasticity of the material (conditional bending strength);  $\sigma_{u.b.}$ , ultimate bending strength;  $\epsilon_{th}$ , theoretical ultimate relative deformation;  $\epsilon_u$ , ultimate relative deformation (measured);  $\epsilon_{t.b.}$ , ultimate relative deformation in bending on the tension surface of the specimen;  $\epsilon_{m.b.}$ , mean (for the tension and compression surfaces) ultimate relative deformation in bending; and  $\sigma_{th}$ , stresses calculated from  $\epsilon_u$  and E.

with Griffith's theory\* viz., that the less elastic energy is stored in the material by the time a crack is formed and the greater the destruction ductility of the material the less it will be damaged by a thermal load:

$$R^{IV} = \frac{E\gamma}{\sigma_u^2} = R^{III}\gamma, \quad (2)$$

where  $\gamma$  is the surface energy of the material. In order to simplify the discussion, the quantity  $(1 - \mu)$  is omitted from the criterion here and elsewhere.

When the values of  $\gamma$  are unknown or the difference between them can be neglected,  $R^{III}$  can be considered an independent criterion of the thermal-shock resistance.

It can be easily shown that the calculation of the energy of elastic deformation  $W = (1/2) \cdot (\sigma_u^2/E)$  in Eq. (2) conforms to Hooke's law.

The physical interpretation of Eq. (2) is based on Griffith's relation between the stress  $\sigma_u$  arising from the instability of the crack and the surface energy  $\gamma$  of the material:

$$\sigma_u = K \sqrt{\frac{\gamma E}{c}},$$

where K is a coefficient which depends on the mode of load application, the geometry of the crack, etc., and c is the critical length of the cracks.

It follows (with a precision to a constant coefficient) that the length of the crack causing destruction is  $c = \gamma E / \sigma_u^2$ , i.e., that it coincides with criterion  $R^{IV}$ .

Thus, when using criterion  $R^{III}$ , the material with the longer critical crack is regarded as better able to resist destruction.

\* W. D. Kingery [8] was the first to apply Griffith's idea for determining the thermal-shock resistance.

TABLE 1. Characteristics of the Tested Materials

No.	Material composition	Apparent porosity, %	Meas. of brittle- ness X	Ult. bending strength, kgf/cm <sup>2</sup>		Ult. rel. deform. $\epsilon_{t, b.} \cdot 10^4$ , rel. units	Elastic modulus E <sup>*</sup> $10^{-6}$ , kgf/cm <sup>2</sup>	Coeff. of linear ex- pansion $\alpha \cdot 10^6$ , 1/ deg C
				$\sigma_{e. b.}$	$\sigma_{t. b.}$			
1	Al <sub>2</sub> O <sub>3</sub> +0,1% MgO (translucent corundum)	0	1	1916	1916	4,75	4,05	11,0
2	Al <sub>2</sub> O <sub>3</sub> +1% TiO <sub>2</sub>	1-2	1	1180	1180	3,55	3,30	6,0
3	Al <sub>2</sub> O <sub>3</sub> +1% TiO <sub>2</sub> +7% $\alpha$ -Al <sub>2</sub> O <sub>3</sub> *	3-4	0,85	649	615	2,65	2,64	6,7
4	Al <sub>2</sub> O <sub>3</sub> +1% TiO <sub>2</sub> +15% $\alpha$ -Al <sub>2</sub> O <sub>3</sub> *	5-6	0,61	676	524	3,10	2,35	7,2
5	Al <sub>2</sub> O <sub>3</sub> +15% ZrSiO <sub>4</sub>	23	0,40	671	470	9,58	0,94	7,6
6	ZrO <sub>2</sub> +4% CaO+4% H <sub>3</sub> PO <sub>4</sub> (unfired refractory)	17	0,38	46	31	3,20	0,19	10,0

\*  $\alpha$ -Al<sub>2</sub>O<sub>3</sub> is present in the form of monocrystalline flakes.

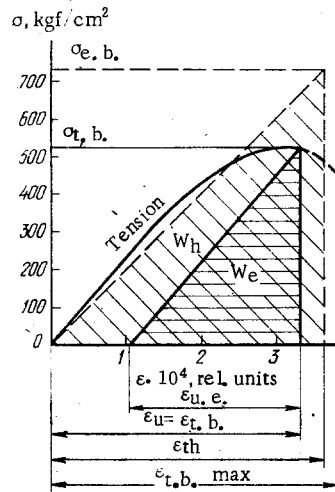


Fig. 2

Fig. 2. Diagram of the deformation in bending of a specimen molded from reinforced corundum (Al<sub>2</sub>O<sub>3</sub> + 1% TiO<sub>2</sub> + 15%  $\alpha$ -Al<sub>2</sub>O<sub>3</sub> flakes): We, effective elastic energy; Wh, hypothetical elastic energy;  $\epsilon_{u. e.}$ , elastic component of the ultimate relative deformation; and  $\epsilon_{t. b. max}$ , ultimate relative deformation recorded up to the instant of destruction of a specimen for which the achievement of the ultimate state on the surface ( $\epsilon_{t. b.}$ ) does not result in loss of carrying capacity.

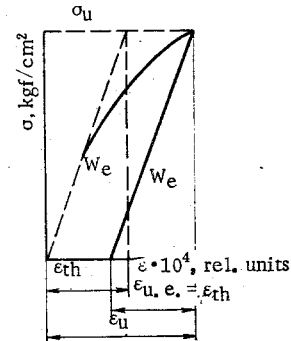


Fig. 3

Fig. 3. Diagram of tensile deformation.

Next, consider the physicomechanical characteristics upon which the criteria concerned here are based. It is well known [3] that they are calculated from the ultimate strength determined in tensile and bending tests in which a discrepancy between these quantities is treated merely as a discrepancy between their absolute values; the difference in the stress conditions of the specimens at the instant of destruction are not taken into account.

Consider the deformation diagrams (the stress-strain relation) of refractories and the methods of obtaining the diagrams. In tensile tests measurements are carried out of the load P and the elongation  $\Delta l$  of the working part of a specimen of length l, or of its relative deformation  $\epsilon$  in the direction of action of the destroying stresses. The tension stress  $\sigma = P/F$ , where F is the cross section of the specimen [9, p. 13], is calculated from the functions  $P = f(\Delta l)$  or  $P = f(\epsilon)$ . The deformation and elongation are linked in the equation  $\epsilon = \Delta l/l$ . This calculation is suited for a linear-elastic material or any other so that the plotting of the deformation diagram is a simple matter.

In bending tests the quantities being measured are similar, i.e., the load P and the deflection  $\delta$  of the specimen or its relative deformation in the direction of action of the destruction stresses ( $\epsilon_{t. b.}$  in the

TABLE 2. Comparative Results of the Assessments of the Thermal-Shock Resistance

Material number (see Table 1)	Thermal-shock resistance criterion defining the resistance of material to cracking, °C		Destructive temp. drop in a hollow cylindrical specimen, deg	Thermal-shock resistance criterion defining the resistance of material to destruction, cm <sup>2</sup> /kg		Thermal shock resistance (1300-20°C) reveals in air	Destruction characteristics of hollow cylindrical specimens
	σ <sub>e. b.</sub>	ε <sub>u</sub>		E	I		
	Eα	α		σ <sub>e. b.</sub>	σ <sub>t. b.</sub> , u.e.		
1	43	43	135	1,1	1,1	1	Catastrophic, the specimen broke up into two or three parts
2	59	59	153	2,4	2,4	1	The specimen broke up into two parts
3	37	39	132	6,3	6,9	8	A continuous and a noncontinuous crack developed in most cases
4	40	43	142	5,1	8,5	12	Only a single continuous crack developed
5	94	126	253	2,1	4,3	5	Ditto
6	24	32	122	89,0	198,0	Not determined	Slow destruction, continuous cracks developed after ΔT was increased by 7-15%

surface under tension and ε<sub>c. b.</sub> in that under compression). The different behavior of the material in bending arises from the fact that in the cross section of the specimen not only is the stress distribution uneven but the signs of the stresses undergo reversal.

It follows therefore that, firstly, only the mean relative deformation can be calculated from the deflection:

$$\varepsilon_{m. b.} = \frac{\varepsilon_{t. b.} + \varepsilon_{c. b.}}{2} = \frac{4h\delta}{(L-2a)^2}$$

where L is the distance between the outer supports, h the height of the specimen, and a the distance between the inner and outer supports. (To obtain more precise theoretical data [10], consider the case of pure bending).

Secondly, there are various approaches to the evaluation of the results of the tests. For linear-elastic materials, e.g., the deformation diagrams (Fig. 1a) are based on the ultimate strength values calculated from the equations of the strength of materials [9]:

$$\sigma_{e. b.} = \frac{3Pz}{bh^2}$$

where b is the width of the specimen.

For inelastic materials this calculation gives only so-called nominal\* deformation diagrams (Fig. 1b) the values of the stresses in which are overstated to the extent that the material is less elastic-deformable [10].

A more general equation, e.g., [11]

$$\sigma_{m. b.} = \frac{2a}{bh^2} \left[ P + \frac{1}{\delta} \frac{dP}{d\delta} \right]$$

is used to determine the actual ultimate strength values of the specimen but they are the mean values because in these equations account is taken of the relation between the deformation and the stresses but not of

\* The diagram (broken line in Fig. 1b) for which the deformation is not measured but calculated in accordance with Hooke's law ε<sub>th</sub> = σ<sub>u</sub>/E can be called "hypothetical." Note that this is not the same as the diagram (broken line, Fig. 1c) for which the stresses σ<sub>th</sub> are calculated from the measured ultimate deformation ε<sub>u</sub> and the elastic modulus E.

the difference between the tensile and compressive deformability of the material (Fig. 1c).

Another approximation to the real picture consists of determining a possible difference in the resistance of the material to tension and compression, e.g., by strain gauge techniques. In this case the deformation diagram (Fig. 1d) is expressed as the variation of the relative tensile deformation in bending  $\epsilon_{t,b.}$  with the destruction stresses on the tension surface of the specimen which can be calculated, e.g., from the following equation:

$$\sigma_{t,b.} = \frac{a}{bh^2} \left[ P + \frac{e_{m,b.} dP}{2de_{m,b.}} \right] \times \left[ 1 + \frac{\frac{dc_{c,b.}}{de_{m,b.}}}{\frac{de_{m,b.}}{d\epsilon_{t,b.}}} \right].$$

Such a diagram will be especially necessary when the specimen in the bending tests does not lose its carrying capacity (Fig. 2) as the ultimate state sets in on its surface because it is on the surface that the effective ultimate relative deformation  $\epsilon_{t,b.}$  corresponding to the disturbance of the equilibrium on the tension surface manifests itself. The descending section of this diagram corresponds to the state when the force of the load increases although the destruction of the specimen has already begun. This phenomenon occurs when the microdestructions in the tension surface layer exceed the permitted limit for the material concerned and the load is taken over by the next layer of the specimen [12].

In a dimensionless assessment of the thermal-shock resistance, an important problem is that of the elastic moduli of the material. They can be the dynamic elastic moduli  $E_{dyn}$  determined from the rate of propagation of ultrasound in the material or from the frequency of its natural oscillations, or the static elastic moduli  $E_{st}$  expressed as the tangent of the angle of inclination of the tangent to the deformation diagram at near-zero stresses. For practical purposes the elastic moduli  $E_{dyn}$  and  $E_{st}$  can be treated as equivalent.

Matters are different with the transversal modulus  $E_{tr}$  which expresses the ratio of the ultimate deformation  $\epsilon_u$  to the ultimate stress  $\sigma_u$  (see Fig. 1). It is well known that for elastic-deformable materials the values of these moduli are identical but for a material which deforms inelastically the transversal modulus may differ very considerably from the real elastic modulus.

In an analysis of the criterion of thermal-shock resistance consider, to begin with, the case in which the characteristics of the materials are determined under a tension load. In the criterion of thermal-shock resistance the ultimate deformations are expressed in terms of Hooke's law and therefore correspond to the actual deformations only for linear-elastic materials. For other materials the theoretical values of the ultimate relative deformation  $\epsilon_{th}$  will be understated (Fig. 3), and the difference between the theoretical and measured values of  $\epsilon_u$  will increase with a decrease in the linearity of the deformation diagram.

It follows that criterion A calculated from the conventional equations will be understated to the extent that the material is inelastic (i.e., that the measure of brittleness  $\chi$  decreases [1]). In other words, the information about the thermal-shock-resistance of the material will be unreliable. One can suggest therefore that the ratio  $\sigma_u/E$  in the A type criteria be replaced by the actual ultimate deformation of the material  $\epsilon_u$ , a step which would be advantageous also for other reasons [13, 14].

In its general form the criterion is then expressed as follows:

$$A_e = \frac{\epsilon_u}{\alpha} B.$$

When the values of the approximate measure  $\chi'$  of the brittleness [1] of the material are known the criterion can be written as follows:

$$A_e = \frac{\sigma_u}{\chi' E \alpha} B.$$

In an analysis of inelastically deforming materials no correction is required for  $R^{IV}$  type criteria since the analytically predicted deformation values (see Fig. 3) coincide with the elastic\* components  $\epsilon_{u,e.}$  of the ultimate deformation of the material. Thus, the quantity  $E/\sigma_u^2$  expresses the reciprocal of the effective unit elastic energy  $W_e$  stored in the material. This is an important parameter.

\* The elastic modulus is assumed to be the same in the load application as in the load removal. This is admissible in the first approximation in tensile and bending tests with refractories.

As in the preceding case, when determining the bending strength of elastically deformable materials the application of Eqs. (1) and (2) presents no problems. In the case of inelastically deforming materials, however, the picture is far from clear. If the A type criteria for these materials are calculated from data relating to the nominal ultimate bending strength  $\sigma_{e.b.}$  and the elastic moduli E, then the picture is similar (see Fig. 1b) to that for a tension load. When the calculations are based on the more precise values of the bending strength  $\sigma_{m.b.}$  or  $\sigma_{t.b.}$  (see Fig. 1c and d) the position is no better because for these materials  $\sigma_{e.b.} > \sigma_{m.b.} > \sigma_{t.b.}$  so that the values of the analytically predicted deformations will be understated to a still greater extent.

The criterion of thermal-shock resistance which defines the ability of brittle and relatively brittle refractories [5] to resist the onset of destruction, must therefore be formulated on the basis of the ultimate relative deformation, i.e., it must be expressed as follows:

$$A_e = \frac{\epsilon_u}{\alpha} B. \quad (3)$$

In the case of refractories with low values of the measure  $\chi$  of brittleness (see Fig. 2) the quantity  $\epsilon_u$  is replaced by  $\epsilon_{t.b.}$  so that criterion R is expressed\* as  $R_e = \epsilon_{t.b.}/\alpha$ .

In a calculation of the R<sup>IV</sup> type criteria from the results of bending tests the inelasticity of the material is a more important factor, the reason being that the elastic energy of deformation ( $W_m = (1/2) \cdot (\sigma_{e.b.}^2/E)$ ) defined as the area of a hypothetical diagram (see the broken line in Fig. 2) may differ significantly from the effective elastic energy  $W_e = (\sigma_{t.b.} \epsilon_{u.e.})/2$  stored in the material up to the instant of destruction (see the triangle formed by heavy lines in Fig. 2) so that the criterion which expresses the ability of the material to resist cracking should be calculated in the case of inelastically deforming refractories (i.e., relatively brittle types for which  $\chi < 1$ ) from the effective stresses and the elastic components of the ultimate deformations and expressed in this form:

$$R_e^{IV} = \frac{\gamma}{\sigma_{t.b.} \epsilon_{u.e.}} = R_e^{III} \gamma.$$

Agreement between the assessment of the thermal-shock resistance on the basis of the proposed criteria and experimental findings was checked out on refractories which differed considerably in their destruction behavior (Table 1). The results of the experimental and analytical determinations of the thermal-shock resistance are given in Table 2.

## CONCLUSIONS

The characteristics of the behavior of the material after the load application must be taken into account in a nondimensional assessment of the thermal-shock resistance.

For materials that are deformed nonlinearly the calculation of the thermal-shock resistance criteria which define the ability of the material to resist cracking must be based on the measured deformation, and that of the criteria which define the ability of the material to resist destruction on the effective elastic energy stored in the material up to the onset of destruction.

## LITERATURE CITED

1. G. A. Gogotsi, *Probl. Prochn.*, No. 10, 26-29 (1973).
2. K. K. Strellov and G. A. Gogotsi, *Ogneupory*, No. 9, 39-47 (1974).
3. K. K. Strellov, G. A. Gogotsi, and G. N. Tretyachenko, *Probl. Prochn.*, No. 6, 17-23 (1974).
4. J. P. Kiehl and G. Valentin, *Brit. Ceram. Soc.*, 4, 3-23 (1968).
5. G. A. Gogotsi, *Probl. Prochn.*, No. 1, 77-82 (1977).
6. G. S. Pisarenko, V. N. Rudenko, G. N. Tretyachenko, et al., *High-Temperature Strength of Materials [in Russian]*, Naukova Dumka, Kiev (1966).
7. D. P. H. Hasselman, *J. Am. Ceram. Soc.*, 52, No. 11, 600-604 (1969).
8. W. D. Kingery, *J. Am. Ceram. Soc.*, 38, No. 1, 3-15 (1955).
9. S. P. Timoshenko, *Strength of Materials [in Russian]*, Nauka, Moscow (1965).
10. G. A. Gogotsi, Ya. L. Grushevskii, and A. A. Kurashevskii, *Ogneupory*, No. 1, 45-50 (1976).
11. A. Naday, *Plasticity and Destruction of Solids [Russian translation]*, IL, Moscow (1954).

\*When basing the calculations on the transversal moduli  $E_{tR} = \sigma_u/\epsilon_u$  determined from diagrams of the type shown in Fig. 1b, then  $R = \sigma_u/E_{tR}\alpha = \sigma_u\epsilon_u/\sigma_u\alpha = R_e$ .

12. I. Ya. Leonov, K. N. Rusinko, and V. A. Panyaev, in: *Complex Deformation of Solids* [in Russian], Ilim, Frunze (1969), pp. 95-107.
13. E. Gugel, *Ber. Dtsch. Keram. Ges.*, **44**, No. 11, 547-553 (1967).
14. C. R. Manning and L. D. Lineback, in: *Surfaces and Interfaces in Glass and Ceramics*, Plenum Press, New York (1974), pp. 473-490.

## EFFECT OF ZINC MELTS AND VAPOR ON FUSION-CAST POTASSIUM FLUOROPHLOGOPITE

B. Kh. Khan, A. G. Malyavin,  
M. K. Malyavina, and E. S. Lugovskaya

UDC 546.161:666.76.022.846.001.5

Micacrystalline fusion-cast materials possess good thermophysical and physicomachanical properties at effective temperatures up to 1000-1200°C [1]. They are produced by pyrogenic synthesis from appropriate compositions.

In this article the results are reported of an analysis of the interaction of a micacrystalline material based on potassium fluorophlogopite with zinc melts and vapor in laboratory conditions and in industrial installations.\* The laboratory tests were conducted by the crucible method at 500, 600, and 1000°C continuously for 192 h. The industrial tests were carried out over a period of 8 months with molten zinc flowing at a temperature of 450-500°C and a speed of 0.5-2 m/sec (dynamic conditions) along the channel of an MDN-6 type installation. Tests were carried out, moreover, in a muffle furnace used for producing zinc oxide; the experimental muffle constructed of a micacrystalline material was installed in place of a graphite-chamotte muffle and used for 216 h at a temperature of 1320-1340 on its outside surface.†

The channels of the MDN-6 installation and the experimental muffle (inside diameter 150 mm, length 300 mm, wall thickness 15 mm) were cast from a micacrystalline material at the Institute of Casting Techniques of the Academy of Sciences of the Ukrainian SSR [2]. The crucibles for the laboratory tests were machined (diam. 40-50 mm, height 50-60 mm) from rough castings on ordinary metalworking machines.

The micacrystalline material concerned contained 41.6% SiO<sub>2</sub>, 11.8% Al<sub>2</sub>O<sub>3</sub>, 26.9% MgO, 0.7% CaO, 9.1% K<sub>2</sub>O, and 10.6% F<sub>2</sub>. The structure of this material is fully crystalline; the flake crystals of potassium fluorophlogopite form cross-shaped, latticed, and sheaflike concretions as well as random intergrowths. The crystals of potassium fluorophlogopite measure 0.2-2.5 mm. The microstructure of the material of the products is shown in Fig. 1a and its macrostructure in Fig. 1b.

The mineral composition (vol. %) of the material was as follows: 85-95% potassium fluorophlogopite K<sub>2</sub>Mg<sub>3</sub>(Si<sub>3</sub>AlO<sub>10</sub>)F<sub>2</sub>, 5-10% glass phase, and about 5% admixtures of other minerals. The glass phase and admixtures filled the interstices between the fluorophlogopite flakes and increased the density of the structure. A distinguishing feature of the structure is the closed porosity between the randomly oriented fluorophlogopite crystals. It accounts for only 10 wt. % of the material while the open porosity does not exceed 0.5-1%.

After the tests the products were studied macroscopically as well as in polished sections and immersion preparations (Table 1).

It was established that in the tests in static and dynamic conditions at 500-1000°C the cast material of the experimental products did not react with zinc melt, vapor, and oxide. Neither the appearance of the crucibles (Fig. 2) nor the phase composition of the material of the crucibles and channel underwent a change. The high density of the fusion-cast material precluded impregnation with the zinc; the inside surface of the channel was coated with an easily removed layer of zinc not more than 0.1 mm in thickness. In the crucibles the solidifying zinc had formed a convex meniscus and was easily extracted which showed that over the range of temperatures used in the tests the micacrystalline material was not wetted by the molten zinc.

\* The work was carried out with the participation of S. G. Tresvyatskii.

† V. A. Trefnyak participated in the channel tests and B. A. Boiko and A. A. Dovgalev in the tests with the experimental muffle.